*Supplementary Information*

# TPN-COF@Fe-MIL-100 composite used as electrochemical aptasensor for detection of trace tetracycline residues

Yubo Meng[1], Yuchun Huang[1], Gailing Huang[2], Yingpan Song[2,*]

[1] *School of Mechanical Engineering, Henan University of Engineering, Zhengzhou, 451191, PR China*

[2] *College of Material and Chemical Engineering, Zhengzhou University of Light Industry, Zhengzhou, 450002, PR China*

* Corresponding authors.

E-mail address: wangpan8624@163.com

## S1. Experimental section

### S1.1 Materials and chemicals

Ferric chloride hexahydrate ($FeCl_3 \cdot 6H_2O$), 1,3,5-benzenetricarboxylic acid (BTC), zinc chloride ($ZnCl_2$) and terephthalonitrile were purchased from Aladdin Reagent Co. Ltd. Dimethylformamide (DMF), and ethanol (EtOH) were obtained from Sinopharm Chemical Reagent Co., Ltd. Ampicillin (AMP), bleomycin (BLM), chlortetracycline hydrochloride (CTC), enrofloxacin (ENR), kanamycin (KAN), oxytetracycline (OTC), tetracycline (TET), and tobramycin (TOB) were obtained from Solarbio Life Sciences Co., Ltd. All the chemicals were of analytical reagent grade and used without further purification. All solutions were prepared with Milli-Q ultrapure water (≥ 18.2 MΩ·cm).

### S1.2 Synthesis of Fe-MIL-100

The synthesis of Fe-MIL-100 was referred to the previous work [1] with slight changes. Briefly, $FeCl_3 \cdot 6H_2O$ (9.8 mmol) was dissolved in 30 mL of DMF to obtain **Solution A**, while BTC (5 mmol) was dissolved in 30 mL of DMF to obtain **Solution B**. The two solutions were separately stirred for 30 min. Then, **Solution B** was slowly dropped into **Solution A**, followed by treating ultrasonically for 30 min. The resulting mixture was then transferred into a Teflon-lined autoclave and heated at 110 °C for 24 h. After that, the product was washed with DMF three times and with ethanol twice, followed by treated in centrifuged at 10000 rpm for 3 min, and then dried in a vacuum oven at 60 °C overnight.

### S1.3 Synthesis of TPN-COF

The synthesis of TPN-COF was according to the reported literature [2]. Typically, terephthalonitrile (1 g) as monomer and $ZnCl_2$ (4 g) as catalyst were placed in a mortar and fully grind. Afterward, the mixture was calcinated in a tube furnace under a $N_2$ flow at 400 °C for 5 h with the heat rate of 5 °C·min$^{-1}$. After cooling to room temperature, the resultant powder was washed with Milli-Q water several times and finally dried under vacuum at 60 °C overnight.

**S1.4 Preparation of solutions**

Phosphate buffer (0.1 M, pH 7.4) was prepared by dissolving 0.242 g of $KH_2PO_4$, 1.445 g of $Na_2HPO_4 \cdot 12H_2O$, 0.200 g of KCl, and 8.003 g of NaCl in 1.0 L of Milli-Q water. The stock solutions of aptamers (1 μM), TET (100 nM), and interferents (AMP, BLM, CTC, ENR, KAN, OTC, and TOB) were prepared with phosphate buffer and stored at 4 °C. The aptamer solutions of different concentrations (10, 20, 50, 100, 200, and 500 nM) were prepared with phosphate buffer and used to study the effect of concentration on sensing performance.

**S1.5 Pre-treatment of Au electrode (AE)**

The bare AE (diameter = 3 mm) was polished with alumina slurry (0.05 μm), followed by washed with the piranha solution ($H_2O_2$ and $H_2SO_4$ in *v*:*v* = 3:7), ethanol, and water for 5 min, successively, and dried under $N_2$ at room temperature. Afterward, the AE was electrochemically activated in 0.5 M $H_2SO_4$ at the potential cycling from −0.2 and 1.6 V, following by rinsed with water and dried under $N_2$.

**S1.6 Electrochemical measurements**

Both electrochemical impedance spectroscopy (EIS) and cyclic voltammetry (CV)

measurements were conducted on the CHI 660E electrochemical workstation (Shanghai Chenhua, China). A conventional three-electrode system was utilized to measure the electrochemical signals for detection with the developed aptasensors, for which the AE modified with different samples, an Ag/AgCl (saturated KCl) electrode, and a platinum slide were utilized as the working, reference, and counter electrodes, respectively. EIS Nyquist plots were obtained in phosphate buffer containing 5 mM $[Fe(CN)_6]^{3-/4-}$, 0.14 M NaCl, and 0.1 M KCl at a potential of 0.21 V, frequency range from 100 kHz to 0.1 Hz, and an amplitude of 5 mV. CV curves were taken in the potential range of −0.2 to 0.8 V at the scan rate of 50 $mV \cdot s^{-1}$. All electrochemical measurements were carried out at ambient conditions. All EIS Nyquist plots were fitted and analyzed using Zview2 software, for which the nonlinear least-squares were fitted to determine the elemental parameters in the equivalent circuit. The typical EIS Nyquist plots and equivalent circuit are shown in **Fig. S1**.

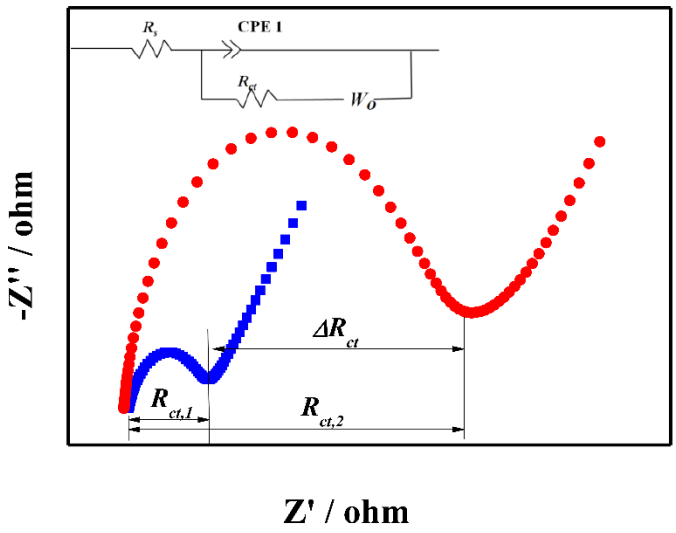


**Fig. S1** Typical EIS Nyquist plots and equivalent circuit.

The sensitivity of aptasensor was evaluated from the LOD. The TPN-COF@Fe-

MIL-100-based aptasensor was separately incubated in TET solutions at different concentrations (0.01, 0.1, 1.0, 10, 100, 1000, and 10000 pg·mL$^{-1}$). By taking the EIS responses (resistance of charge transfer, $R_{ct}$) as the function of logarithm of TET concentration, the calibration curve was achieved, from which the LOD was calculated according to International Union of Pure and Applied Chemistry (IUPAC).

For assessing the selectivity of the TPN-COF@Fe-MIL-100-based aptasensor, different antibiotics (AMP, BLM, CTC, ENR, KAN, OTC, and TOB), which may coexist with TET in milk, were used as the interferents, with a concentration of 1.0 pg·mL$^{-1}$, which is 100-fold of TET (10 fg·mL$^{-1}$). The regenerability of aptasensor was performed by soaking TET/Apt/TPN-COF@Fe-MIL-100/AE in 1.0 M NaOH at room temperature for 5 min, and then rinsed with phosphate buffer. Afterward, the electrode was incubated with the TET solution (10 fg·mL$^{-1}$) again until the $R_{ct}$ value returned to the origin level. The same procedure was repeated by several cycles. The EIS responses of TET/Apt/TPN-COF@Fe-MIL-100/AE was continuously tested for 15 days to investigate the stability of aptasensor. Further, five Apt/TPN-COF@Fe-MIL-100/AEs were independently used to detect TET for evaluation of the reproducibility by EIS technique.

Herein, milk was selected as the real sample. In a 50.0 mL centrifuge tube, 12.0 mL of raw milk was mixed with 18.0 mL of ultrapure water and 6.0 mL of a mixture of 10% trichloroacetic acid and chloroform by vortexing for 1 min to deposit protein and dissolve organic substances in the matrix. The mixture was then ultrasonically treated for 15 min at 20 °C and centrifuged at 13,000 rpm for 10 min to separate the deposition.

The supernatant was transferred into another centrifuge tube and was centrifuged at 10,000 rpm for 10 min to again remove the deposition. A certain amounts of TET was added into the raw liquid milk and was then pretreated and analyzed in accordance with the aforementioned procedure. The final solution was used to detect TET in accordance with the proposed method.

**S1.7 Characterization**

Field emission scanning electron microscope (FE-SEM) was carried out on JSM-6490LV. X-ray diffraction (XRD) patterns were measured on a Rigaku D/Max-2500 X-ray diffractometer (Cu $K_\alpha$ radiation). Fourier transform infrared (FT-IR) spectra were collected on a Bruker TENSOR27 spectrometer. Raman spectra were performed on a LabRAM HR Evolution Raman spectrometer (633 nm). X-ray photoelectron spectroscopy (XPS) was taken by an AXIS HIS 165 spectrometer (Kratos Analytical) with a monochromatized Al $K_\alpha$ X-ray source (1486.71 eV photons). The specific surface areas of all samples were carried out by the method of Brunauer-Emmett-Teller (BET) using a Micromeritics ASAP2022 instrument at the temperature of liquid nitrogen. Prior to each measurement, the samples were degassed at 573 K for 8 h.

## S2. Nitrogen adsorption and desorption measurements

Brunauer-Emmett-Teller (BET) surface area analysis was employed to investigate the porosity for the three samples. The $N_2$ adsorption-desorption isotherms of the three samples were obtained (**Fig. S2a**). It displays that the specific surface areas of TPN-COF, Fe-MIL-100 and TPN-COF@Fe-MIL-100 are calculated to be 2.74, 54.36, and 68.95 $m^2 \cdot g^{-1}$, respectively. As shown in the pore size distribution (**Fig. S2b**), the average pore diameters of TPN-COF, Fe-MIL-100 and TPN-COF@Fe-MIL-100 are evaluated to be 0.5, 11.7, and 12.6 nm, respectively. The pore size distribution clearly reveals that the majority of pores for Fe-MIL-100 and TPN-COF@Fe-MIL-100 are in the mesoporous region, while the majority of pores for TPN-COF is in the microporous region. Typically, the nitrogen adsorption by the mesopores is much higher than that of micropores. All of these results indicate that the TPN-COF@Fe-MIL-100 is feasible to disperse in the aqueous solution and easy to employ as the scaffold for the immobilization of probe molecules owing to its high specific surface area and relatively larger mesopores.

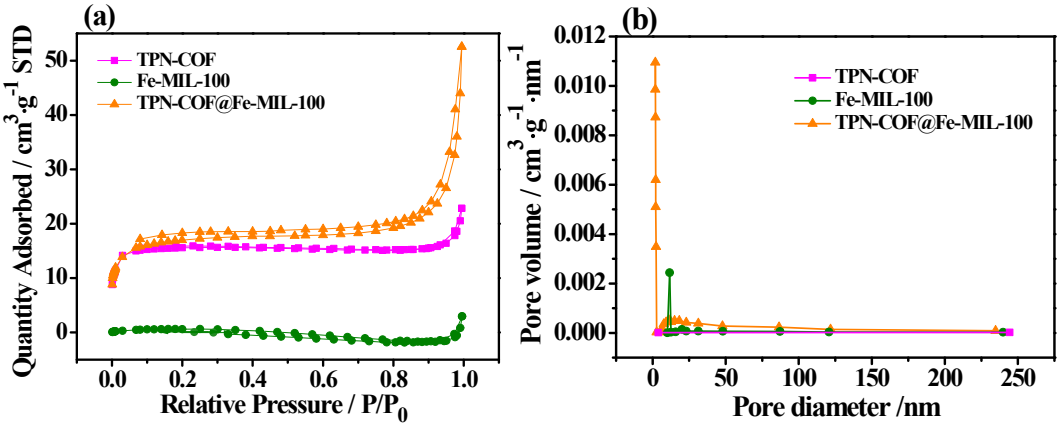


**Fig. S2** (a) Nitrogen adsorption-desorption isotherm, and (b) pore size distribution of TPN-COF, Fe-MIL-100 and TPN-COF@Fe-MIL-100.

## S3. Electrochemical TET sensing performance of TPN-COF@Fe-MIL-100-based aptasensor

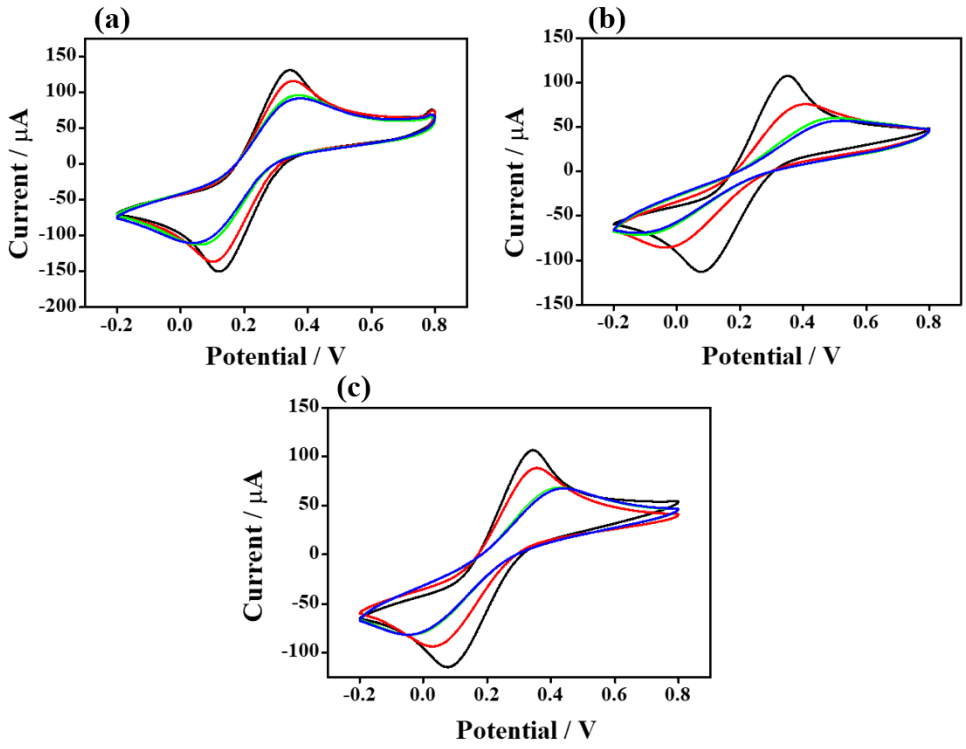


**Fig. S3** CV curves of the aptasensor based on (a) Fe-MIL-100, (b) TPN-COF, and (c) TPN-COF@Fe-MIL-100 for detecting TET (10 fg·mL$^{-1}$), including (i) bare AE, (ii) material/AE, (iii) Apt/material/AE, and (iv) TET/Apt/material/AE. Conditions: 5.0 mM $[Fe(CN)_6]^{3-/4-}$ in 0.1 M phosphate buffer + 0.14 M NaCl + 0.1 M KCl ($n$ = 3).

**Table S1** $R_{ct}$ values for each step during the fabrication procedures of different aptasensors based on Fe-MIL-100, TPN-COF, and TPN-COF@Fe-MIL-100 for detection of TET.

| Electrode materials | $R_{ct}$ (Ω) | | | |
|---|---|---|---|---|
| | Bare AE | Modified AE | Aptamer immobilization | TET detection |
| **Fe-MIL-100** | 170 | 350 | 490 | 630 |
| **TPN-COF** | 84 | 206 | 400 | 520 |
| **TPN-COF@Fe-MIL-100** | 100 | 430 | 650 | 830 |

**Table S2** Corresponding variations in $R_{ct}$ values for each step during the fabrication procedures of different aptasensors based on Fe-MIL-100, TPN-COF, and TPN-COF@Fe-MIL-100 for detection of TET.

| Electrode materials | $\Delta R_{ct}$ (Ω) | | |
|---|---|---|---|
| | $R_{ct,\ material} - R_{ct,\ AE}$ | $R_{ct,\ Apt} - R_{ct,\ material}$ | $R_{ct,\ TET} - R_{ct,\ Apt}$ |
| **Fe-MIL-100** | 180 | 140 | 140 |
| **TPN-COF** | 122 | 194 | 120 |
| **TPN-COF@Fe-MIL-100** | 330 | 220 | 180 |

The core-level XPS spectra of the main elements contained in the TPN-COF@Fe-MIL-100 after aptamer binding and sensing the TET analyte were fitted out and are summarized in **Fig. S4**. As for the C 1s core-level XPS spectra (**Figs. S4a** and **c**), four kinds of peaks at 284.6, 285.7, 286.4, and 287.7 eV, were fitted out, which are assigned to C–C, C–N, C–O, and C=O/N–C=O groups, respectively. Among them, the relatively high content of the C=O/N–C=O group for Apt/TPN-COF@Fe-MIL-100 was a result of the anchored aptamer strands (**Fig. S4a**); however, its content decreased after TET was detected (**Fig. S4c**). Since aptamer strands contain $–PO_4^–$ in their base pairs, the successful adsorption of aptamer strands also can be proven by the presence of the P 2*p* signal in the two samples (**Figs. S4b** and **d**). The P 2*p* core-level XPS spectra can be deconvoluted into two parts at 132.4 and 134.8 eV because of the presence of P $2p_{3/2}$ and P $2p_{1/2}$ (**Fig. S4b**) [3]. Besides, the binding energies of P 2*p* in TET/Apt/TPN-COF@Fe-MIL-100 (**Fig. S4d**) shows no change, which suggested that the Apt/TPN-COF@Fe-MIL-100 retains its original structure when detecting TET.

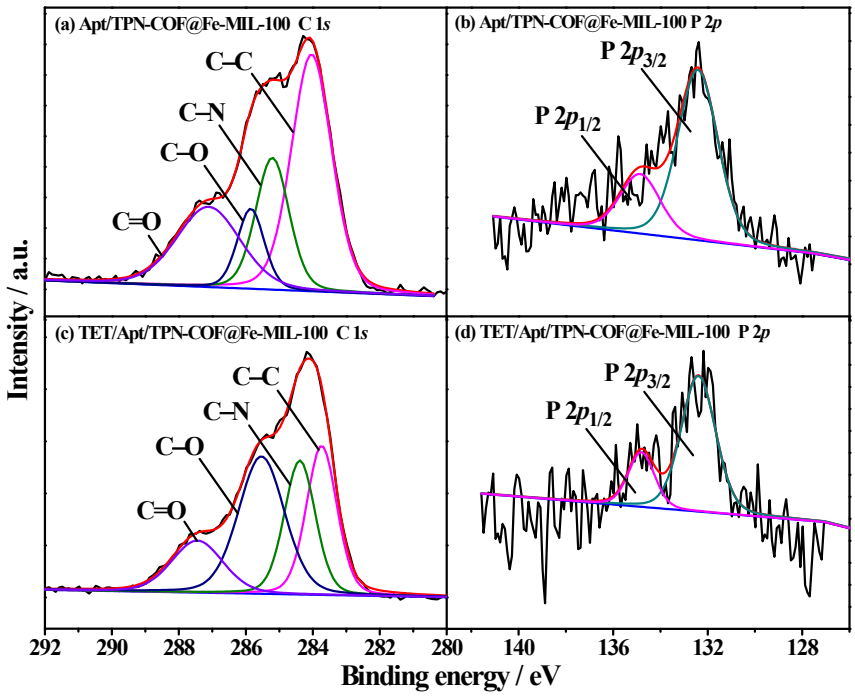


**Fig. S4** High-resolution XPS spectra of (a, c) C 1*s* and (b, d) P 2*p* of (a, b) Apt/TPN-COF@Fe-MIL-100 and (c, d) TET/Apt/TPN-COF@Fe-MIL-100.

## S4. Optimization of parameters for detecting TET

Different concentrations of TPN-COF@Fe-MIL-100 were used to evaluate the sensing performance of the aptasensor. As shown in **Fig. S5a**, the $\Delta R_{ct}$ values increase with increasing the concentrations of TPN-COF@Fe-MIL-100, indicating that more sensing materials are covered on the surface of AE. Meanwhile, the amount of aptamer immobilization and TET detection also increase with the loading of TPN-COF@Fe-MIL-100. The maximum $\Delta R_{ct}$ value can be gained at 1.0 mg·mL$^{-1}$ of TPN-COF@Fe-MIL-100, owing to excessive sensor layer thickness [4]. Thus, 1.0 mg·mL$^{-1}$ of TPN-COF@Fe-MIL-100 dispersion was selected to develop the aptasensor.

The optimization of aptamer concentration and incubation time were also taken by EIS. As shown in **Fig. S5b**, the concentration of aptamer is from 10 to 500 nM, where $\Delta R_{ct}$ values increase with increasing aptamer concentration until reaching steady state. It is because that saturated adsorption aptamer layer on the sensitive electrode surface might block further adsorption of aptamer due to electrostatic repulsion interaction [4]. Consequently, the optimal concentration of aptamer solution was chosen as 100 nM. The incubation time of aptamer is closely associated with the effectiveness of the aptasensor. In **Fig. S5c**, the effect of anchoring time for aptamer was studied and the $R_{ct}$ value arrives a maximum after incubating 80 min. As such, the optimized incubation time of 80 min was utilized in this experiment.

The EIS responses for detecting TET at different pH values were also studied for the TPN-COF@Fe-MIL-100-based aptasensor. The corresponding $\Delta R_{ct}$ values were calculated from the equivalent circuit (**Fig. S5d**). The $\Delta R_{ct}$ value increases with the pH

values changes from 5.0 to 7.4. As the pH value further increases, the $\Delta R_{ct}$ value decreases due to the possible denaturation of aptamers. Therefore, the optimal pH value of 7.4 for detecting TET was selected for further measurements.

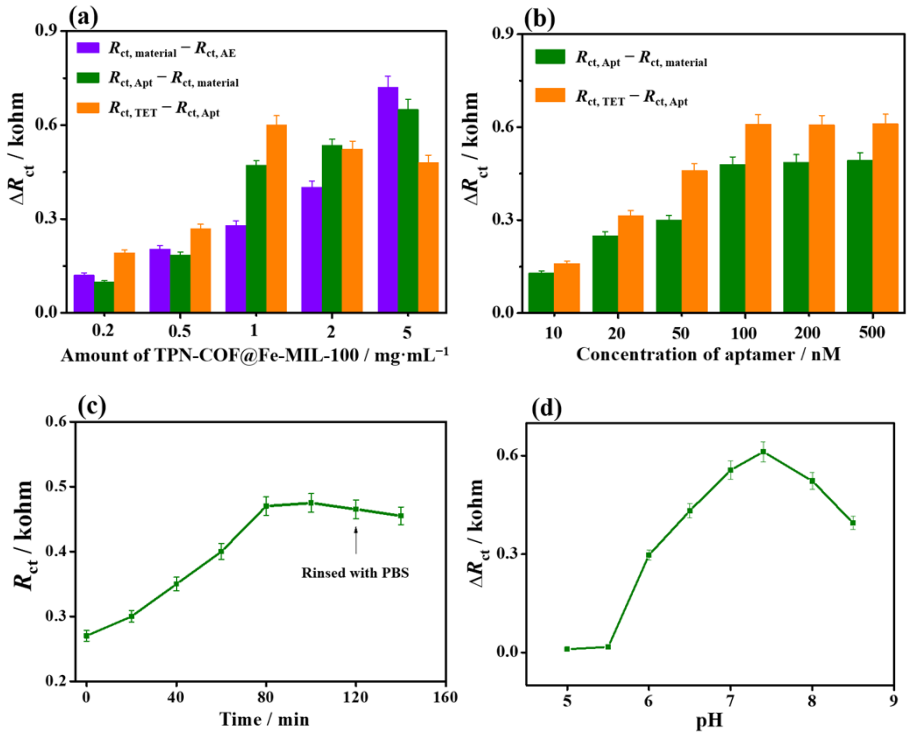


**Fig. S5** (a) The effect of TPN-COF@Fe-MIL-100 amounts on aptasensor fabrication and TET detection, as represented by $\Delta R_{ct}$ values for each step. (b) Variations in $R_{ct}$ for each stage during the fabrication procedure of TET aptasensors using different aptamer concentrations. (c) The corresponding $\Delta R_{ct}$ values for immobilizing aptamer recorded at different aptamer incubation times. (d) Effect of pH value on TET detection, as illustrated by $\Delta R_{ct}$ values for TET detection. Conditions: 5.0 mM $[Fe(CN)_6]^{3-/4-}$ in 0.1 M phosphate buffer + 0.14 M NaCl + 0.1 M KCl ($n$ = 3).

As for the regenerability test of the TPN-COF@Fe-MIL-100-based aptasensor, Apt/TPN-COF@Fe-MIL-100 was successively soaked in TET solution and rinsed TET with phosphate buffer for several cycles. During the test, XRD patterns were also used to investigate the stability of Apt/TPN-COF@Fe-MIL-100 when detecting TET (**Fig. S6**). Obviously, after separately detecting TET for 3, 6, and 9 cycles, the XRD patterns of Apt/TPN-COF@Fe-MIL-100 (i.e., after rinsed TET of TET/Apt/TPN-COF@Fe-MIL-100 with phosphate buffer) are similar with that of pristine Apt/TPN-COF@Fe-MIL-100, indicating that Apt/TPN-COF@Fe-MIL-100 can retain its crystalline structure and keep its stability for detecting TET during a long period and after several cycles.

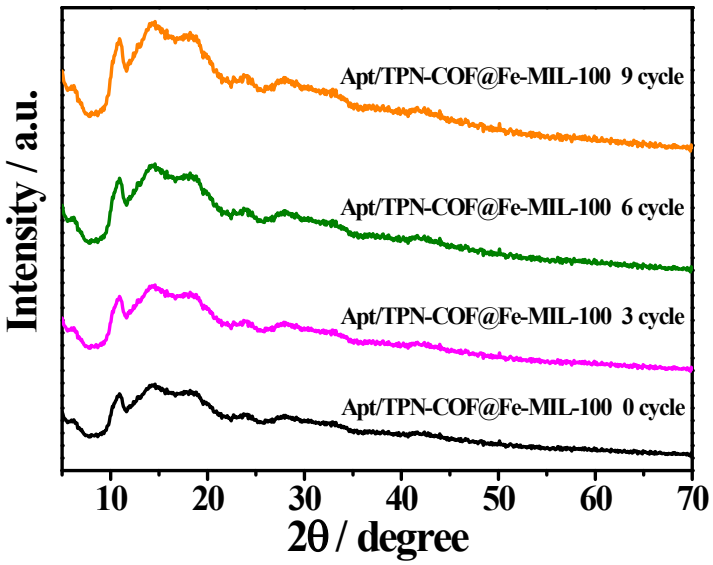


**Fig. S6** XRD patterns of Apt/TPN-COF@Fe-MIL-100 for detecting TET after several cycles.

## References

1 M. Tong, D. Liu, Q. Yang, S. Devautour-Vinot, G. Maurin and C. Zhong, *J. Mater. Chem. A*, 2013, **1**, 8534-8537.

2 P. Kuhn, A. Forget, D. Su, A. Thomas and M. Antonietti, *J. Am. Chem. Soc.*, 2008, **130**, 13333-13337.

3 Z. Zhang, H. Ji, Y. Song, S. Zhang, M. Wang, C. Jia, J. Tian, L. He, X. Zhang and C. Liu, *Biosensors and Bioelectronics*, 2017, **94**, 358-364.

4 L. He, Z. Li, C. Guo, B. Hu, M. Wang, Z. Zhang and M. Du, *Sensor. Actuat. B-Chem.*, 2019, **298**, 126852.